Structural Manipulation of Benzofulvene Derivatives Showing Spontaneous Thermoreversible Polymerization. Role of the Substituents in the Modulation of Polymer Properties

Andrea Cappelli,*,† Simone Galeazzi,† Germano Giuliani,† Maurizio Anzini,† Alessandro Donati,‡ Lucia Zetta,§ Raniero Mendichi,§ Marianna Aggravi,‡ Gianluca Giorgi,⊥ Eugenio Paccagnini,# and Salvatore Vomero†

Dipartimento Farmaco Chimico Tecnologico and European Research Centre for Drug Discovery and Development, Università degli Studi di Siena, Via A. Moro, 53100 Siena, Italy; Dipartimento di Scienze Chimiche e dei Biosistemi, Università degli Studi di Siena, Via A. Moro, 53100 Siena, Italy; Istituto per lo Studio delle Macromolecole (CNR), Via E. Bassini 15, 20133 Milano, Italy; Dipartimento di Chimica, Università di Siena, Via A. Moro, 53100 Siena, Italy; and Dipartimento di Biologia Evolutiva, Università di Siena, Via A. Moro, 53100 Siena, Italy

Received December 20, 2006; Revised Manuscript Received February 26, 2007

ABSTRACT: The synthesis of a series of benzofulvene derivatives **3** related to the recently studied ethyl 1-methylene-3-(4-methylphenyl)-1*H*-indene-2-carboxylate (**BF1**) is described. The properties of these *trans*-diene derivatives were characterized with regard to their capability of polymerizing spontaneously to give new polymers based on functionalized indene monomeric units. The series of polymers has been investigated by NMR spectroscopy, multiangle light scattering online to size exclusion chromatography, UV−vis spectroscopy, mass spectrometry, differential scanning calorimetry, and scanning electron microscopy. The new polymers show very interesting properties such as a thermoreversible polymerization/depolymerization, a variable degree of π-stacking, a tendency to give nanostructured macromolecular aggregates, and a high solubility in the most common organic solvents. Remarkably, this study demonstrated that most of the polymer properties (e.g. formation, molecular weight, structure, thermoreversibility, and aggregation in nanostructured entities) may be modulated by the stereoelectronic characteristics of the substituents present on the indene moiety.

1. Introduction

In the chemistry of advanced materials, the synthesis of vinyl polymers possessing stable, regulated π-stacked conformations represents an important objective, and in this context, the properties of polydibenzofulvene derivatives (e.g., poly-**DBF**) are now being largely investigated.[1−7] Very interestingly, poly-**DBF** is a new synthetic "π-way" molecule showing a hole drift mobility only slightly lower than that of Se,[8] an inorganic semiconductor, but it has been reported to show poor solubility and miscibility with other polymers.[1,2,6]

As thermoreversible polymerization processes are capable of potentially providing materials possessing varied and unique utility (e.g., recyclable materials), the study of the properties of thermally reversible polymers can be considered an interesting research issue.[9]

A survey of the literature showed that several dibenzofulvene polymers have been reported, while only one polymer based on the 3-phenylbenzofulvene structure has been described (poly-**BF2**).[10]

We have recently reported that benzofulvene derivative **BF1** [ethyl 1-methylene-3-(4-methylphenyl)-1*H*-indene-2-carboxylate, Scheme 1] undergoes spontaneous polymerization to give poly-**BF1**, a polymer showing outstanding properties such as thermoreversible polymerization/depolymerization behavior, high solubility in the most common organic solvents, susceptibility to molecular manipulation, and characterized by both a vinyl structure stabilized by aromatic stacking interactions and a very high molar mass.[11,12]

Moreover, transmission electron microscopy (TEM) revealed that this interesting polymer is liable to give nanostructured macromolecular aggregates.

However, the synthesis of poly-**BF1** involved the reaction of the appropriate indenone derivative with methylmagnesium bromide to give the corresponding indenol derivative in low yield (31%),[11] and the general applicability of the synthetic method to the preparation of novel polymers has not been investigated.

A functionalized polymer structurally related to poly-**BF1** has been shown to release the bioactive monomer (**BF-AT1**, an angiotensin II AT_1 receptor antagonist) with temperature-dependent kinetics until the establishment of a temperature-dependent equilibrium such as occurs in the equilibrium polymerization processes. The results of binding studies performed on this polymer strongly support the exploration of the potentiality of the thermoreversible polymerization mechanism in drug-controlled release from new polymeric prodrugs.[13]

Therefore, the object of the research described in this paper was to provide a viable general method for the synthesis of novel benzofulvene derivatives properly functionalized in the key positions of the indene moiety in order to investigate on the effects of substituent's features on the polymer properties such as formation, molecular weight, structure, thermoreversibility, and aggregation in nanostructured assemblies.

* Corresponding author: Tel +39 0577 234320; Fax +39 0577 234333; e-mail cappelli@unisi.it.

† Dipartimento Farmaco Chimico Tecnologico and European Research Centre for Drug Discovery and Development, Università degli Studi di Siena.

‡ Dipartimento di Scienze Chimiche e dei Biosistemi, Università degli Studi di Siena.

§ Istituto per lo Studio delle Macromolecole (CNR).

⊥ Dipartimento di Chimica, Università di Siena.

Dipartimento di Biologia Evolutiva, Università di Siena.

10.1021/ma0629236 CCC: $37.00
Published on Web 03/30/2007

Scheme 1

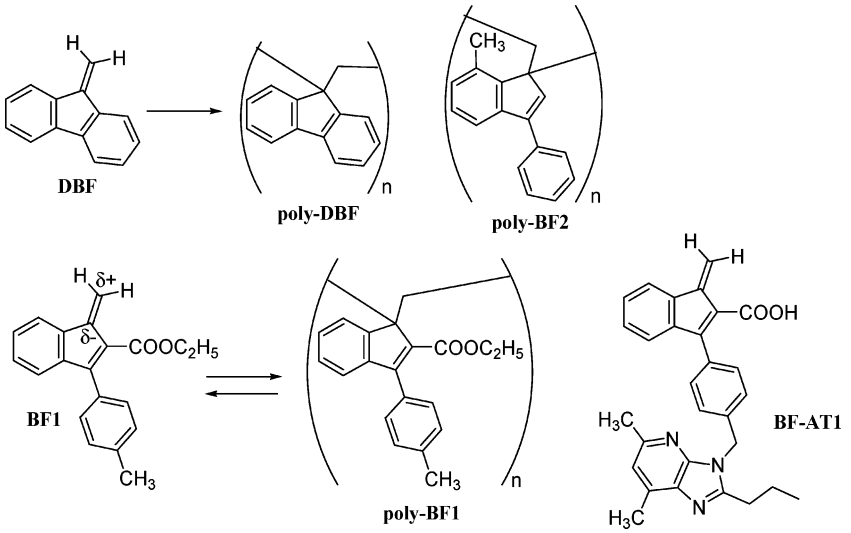

Scheme 2. Synthesis of Novel Benzofulvene Derivatives 3a,c−l,ma,n,o[a]

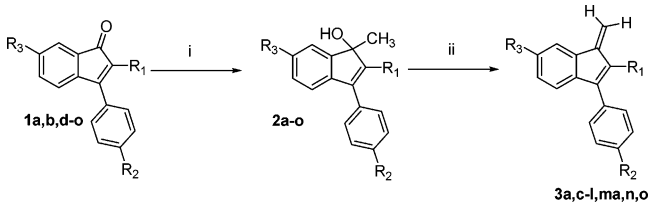

[a] Reagents: (i) $Al(CH_3)_3$, CH_2Cl_2; (ii) PTSA, $CHCl_3$ (or HCOOH for **2j**).

2. Results and Discussion

2.1. Synthesis of the Benzofulvene Monomers. A viable general method for the synthesis of novel benzofulvene monomers bearing different substituent in key positions of the indene moiety is reported in Scheme 2.

The reaction of indenone derivatives **1a,b,d-o** with trimethylaluminium gave the expected indenol derivatives **2a,b,d-o** (the structure of 1,2-addition products **2f,j,m** was solved by X-ray diffraction). The C-methylation of indenone derivatives **1** with trimethylaluminium represents an outstanding improvement in the synthesis of indenol derivatives **2** because the yields are higher (typically 67−94%) with respect to those obtained by means of other standard methods, and in most cases, the indenol derivative could be used in the following step of the synthesis without any further purification.

Dehydration of compounds **2** with *p*-toluenesulfonic acid (PTSA) in chloroform gave compounds of difficult isolation because, in most cases, the solvent removal led to the isolation of polymeric materials containing only trace amounts of the expected *trans*-diene derivatives **3**. When the dehydration was performed in $CDCl_3$, allowing the ^1H NMR analysis to be performed without the solvent elimination, clear ^1H NMR spectra compatible with the structures of **3a,c-l,ma,n,o** were obtained. The dehydration of **2b** led to **3a** because **2b** desilylated spontaneously in the dehydration conditions, and indenol **2m** cleaved spontaneously in the dehydration conditions leading to **3ma**.

The dehydration of indenol **2j** was carried out with formic acid instead of PTSA (Scheme 2) because the latter led to the formation of several byproducts.

The required indenone derivatives were prepared according to the methods described (see Table 1) or by means of the reaction sequences reported in the Supporting Information (Schemes 1SI−5SI).

Finally, the mixture of (ca. 2:1) *E* and *Z* isomers of ω-methylbenzofulvene derivative **3p** was prepared from indenone **1l** via the corresponding ethylindenol derivative **2p** (Scheme 3).

2.2. Formation of Polybenzofulvene Derivatives by Spontaneous Polymerization of Benzofulvene Monomers 3. The diene derivatives **3** were quite stable in solution but polymerized upon solvent removal to give the corresponding polymers (poly-**3**), with the exception of **3n,p**, which did not show a tendency to spontaneous polymerization. On the other hand, poly-**3o** was obtained only in trace amounts by following the same procedure used for the other polymers.

At first sight, these results appeared to indicate that the volume of the substituents in position 2 of the indene moiety affects the formation of poly-**3** by spontaneous polymerization, but comparison of the behavior of benzofulvene derivatives **3g** (R_1 = −C≡N), **3j** (R_1 = −C≡C-2-Pyr) and **3o** [R_1 = CON-$(CH_3)_2$] suggests that the steric hindrance at position 2 of the indene moiety plays a more important role than the total volume of R_1 substituent in inhibiting spontaneous polymerization. In fact, monomer **3j** polymerized spontaneously in spite of the total volume of its R_1 substituent because the presence of the alkynylene spacer displaces the hindrance from position 2. The lack of tendency to polymerize shown by the isomers of ω-methylbenzofulvene derivative **3p** can be considered an interesting support to the previously proposed initiation mechanism for the spontaneous polymerization of **BF1** (**3l**) that is based on the interaction of the strongly polarized exocyclic double bonds of two **BF1** molecules.[12] The presence of a methyl on **3p** activated methylene would prevent the interaction and the consequent formation of the zwitterionic intermediate, which is believed to initiate the spontaneous polymerization. From the thermodynamics point of view, this result can be explained with the high steric crowding of the ethylene moiety leading to a very low ceiling temperature, which prevents the propagation step.

Finally, the lack of spontaneous polymerization in the case of hindered amide derivative **3n** made the structure determination of the complex **3n**-PTSA possible, which showed the H-bonding between amide carbonyl oxygen of **3n** and $-SO_3H$ and the interaction of electropositive vinylene moiety with the π-orbital of PTSA (Figure 1). The distance between the centroid

Table 1. Compounds Shown in Scheme 2

R_1	R_2	R_3	indenone	preparation	indenol (yield)	monomer	polymer (yield)
H	H	H	**1a**	ref 14	**2a** (87%)	**3a**	poly-**3a** (72%)
$Si(CH_3)_3$	H	H	**1b**	ref 14	**2b** (83%)	**3a**[a]	poly-**3a** (72%)
F	H	H			**2c** (36%)[b]	**3c**	poly-**3c** (82%)
Cl	H	H	**1d**	Scheme 1SI	**2d** (84%)	**3d**	poly-**3d** (77%)
Br	H	H	**1e**	ref 14	**2e** (92%)	**3e**	poly-**3e** (58%)
CH_3	H	H	**1f**	Scheme 2SI	**2f** (67%)	**3f**	poly-**3f** (60%)
CN	H	H	**1g**	ref 15	**2g** (94%)	**3g**	poly-**3g** (82%)
CN	CH_3	H	**1h**	Scheme 3SI	**2h** (84%)	**3h**	poly-**3h** (90%)
CN	H	CH_3	**1i**	Scheme 3SI	**2i** (86%)	**3i**	poly-**3i** (87%)
C≡C-2-Pyr	H	H	**1j**	Scheme 2SI	**2j** (79%)	**3j**[c]	poly-**3j** (55%)
$COOC_2H_5$	H	H	**1k**	ref 16	**2k** (82%)	**3k**	poly-**3k** (73%)
$COOC_2H_5$	CH_3	H	**1l**	ref 11	**2l**[d] (82%)	**3l**	poly-**3l** (78%)
$COOC(CH_3)_3$	CH_3	H	**1m**	ref 13	**2m** (75%)	**3ma**[e]	poly-**3ma** (74%)
$CON(CH_3)_2$	CH_3	H	**1n**	Scheme 5SI	**2n** (83%)	**3n**	
$C(CH_3)_3$	H	H	**1o**	ref 14	**2o** (77%)	**3o**	poly-**3o** (2%)

[a] Compound **3a** was obtained instead of **3b** because indenol derivative **2b** desilylated spontaneously in the dehydration conditions. [b] Indenol **2c** was prepared from **2e** as shown in the Supporting Information (Scheme 4SI). [c] Indenol **2j** was dehydrated with formic acid instead of PTSA. [d] Indenol **2l** was previously prepared by a less efficent methodology (yield 31%, see ref 11). [e] Acid **3ma** was obtained instead of *tert*-butyl ester **3m** because indenol derivative **2m** cleaved spontaneously in the dehydration conditions.

Scheme 3. Preparation of Benzofulvene 3p[a]

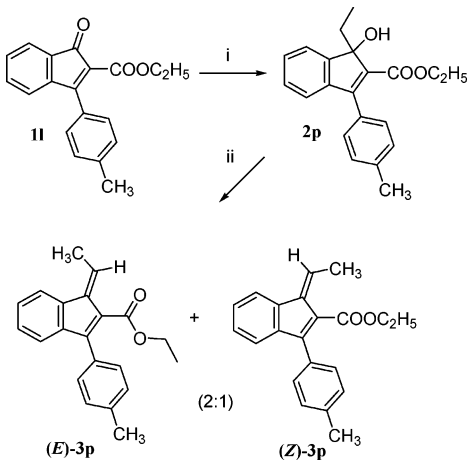

[a] Reagents: (i) $Al(C_2H_5)_3$, CH_2Cl_2; (ii) PTSA, $CDCl_3$ or $CHCl_3$.

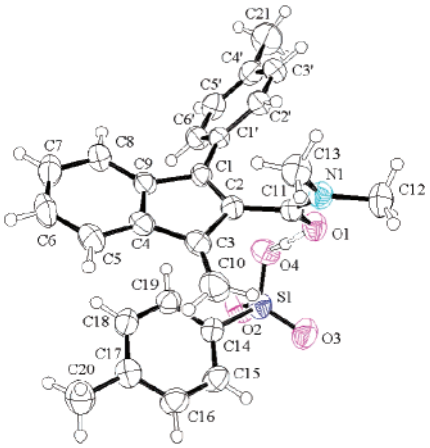

Figure 1. Crystal structure of the complex between benzofulvene derivative **3n** and PTSA.

of PTSA toluene ring and C(10) of **3n** is 3.802 Å. The evidence of this particular cation−π interaction can be considered as an input in the refinement of the proposed initiation mechanism,[12] in view of the fact that a similar interaction between the activated methylene group and the indene π-orbital could be the basis for the formation of the postulated zwitterionic dimer.

2.3. Molecular Weight. The characterization of polymers poly-**3a,c**−**l,ma** by a multiangle laser light scattering on-line to a size exclusion chromatography (SEC-MALS) system gave molecular weight values ranging from about 4.0 to 2670 kg/mol and variable dispersity indexes (see Table 2). Interestingly, the molecular weight, and, consequently, the average number of monomeric units forming a polymer molecule appeared to be roughly related to the steric hindrance in the close proximity of position 2 of the indene nucleus rather than to the volume of substituent R_1.

In particular, the values were found to be high when R_1 was a steric hindering group such as an ester (poly-**3k,l**) and decreased with the decreasing of the size until it became minimum for poly-**3a** where R_1 is a hydrogen atom. Taking together this piece of evidence and the previously proposed initiation mechanism,[12] it is reasonable to assume that the size of the R_1 substituent affects the first step of polymerization, which competes with the propagation process. Thus, a small-sized substituent should facilitate the interaction between two monomers, leading to the formation of a large number of zwitterionic dimer initiators producing low-molecular-weight polymers. On the contrary, a large-sized substituent should be unfavorable for the formation of dimer initiators, facilitating the propagation step and leading to a high-molecular-weight polymer.

2.4. Structure. 2.4.1. NMR. The structure of the newly synthesized polymers was investigated with NMR spectroscopy by performing 1D (^1H, ^{13}C) and 2D (HSQC) experiments on the whole set of the polymers.

The simplest situation was found for poly-**3k**, which resulted to be very similar to the previously described poly-**BF1** (poly-**3l** in the present work). ^{13}C NMR spectra of poly-**3k,l** showed a single peak attributable to the aliphatic quaternary carbon with a chemical shift value (about 58 ppm) close to both the one reported for poly-**BF2** (57.8 ppm) and the one calculated for poly-**BF1** in the 1,2-enchainment (54.2 ppm) (Table 3). Moreover, the broad peak centered at 48.4 ppm attributed to the methylene bridge of poly-**BF1** was resolved in the spectra of both polymers (poly-**3k,l**) into two broad peaks (at about 48 and 51 ppm), showing different intensity and suggesting the contemporary presence of a minor species (m) with a major one (M). The comparison of the chemical shifts of these two broad peaks with that found in the case of poly-**BF2** (43.8 ppm) and with those calculated for the 1,2-enchainment (45.6 ppm) and the 1,4-enchainment (30.2 ppm) of poly-**BF1** supports the vinyl nature (1,2-enchainment) of poly-**3k,l** and suggests the possible existence of configurational or conformational isomers.

Table 2. Macromolecular Features of the Synthesized Polymers

polymer	R_1	R_2	R_3	M_w (kg/mol)[a]	D[b]	R_g (nm)[c]
poly-**3a**	H	H	H	4.0	1.3	
poly-**3c**	F	H	H	25.6	4.5	
poly-**3d**	Cl	H	H	47.6	2.1	
poly-**3e**	Br	H	H	109.1	3.1	
poly-**3f**	CH_3	H	H	530.8	4.7	43.0
poly-**3g**	CN	H	H	391.5	6.3	32.5
poly-**3h**	CN	CH_3	H	500.2	4.4	26.8
poly-**3i**	CN	H	CH_3	475.9	4.3	24.3
poly-**3j**	C≡C-2-Pyr	H	H	289.2	2.5	
poly-**3k**	$COOC_2H_5$	H	H	1593.0	3.7	44.6
poly-**3l** (poly-**BF1**)	$COOC_2H_5$	CH_3	H	2670.0	1.6	
poly-**3ma**	COOH	CH_3	H	694.9	9.6	

[a] M_w = weight-average molecular weight. [b] D = the dispersity index; $D = M_w/M_n$, where M_n denotes the number-average molecular weight. [c] R_g = the radius of gyration, i.e., the dimension of the macromolecules.

Table 3. Significant NMR Features of the Synthesized Polymers

polymer	R_1	R_2	R_3	aliphatic quaternary ^{13}C NMR n[a]	aliphatic quaternary ^{13}C NMR (ppm)[b]	backbone CH_2 HSQC n[c]	backbone CH_2 ^{13}C NMR (ppm)[d]
poly-**3a**	H	H	H	2 broad	55.4, 57.4	>6	33.0−61.0
poly-**3c**	F	H	H	3	49.7 (M)	5	32.8
					50.9 (m)		40.0
					54.0 (m)		42.7
							44.5
							46.1
poly-**3d**	Cl	H	H	4	56.6 (M)	5	37.2
					56.8 (M)		38.8
					57.7 (m)		42.0
					59.9 (m)		44.5
							47.7
poly-**3e**	Br	H	H	2	58.1 (M)	4	39.3
					61.0 (m)		42.8
							45.8
							48.1
poly-**3f**	CH_3	H	H	2	57.4	2	30.0
					61.0		37.2
poly-**3g**	CN	H	H	4	56.5 (M)	5	37.6
					57.7 (m)		39.6
					59.6 (m)		42.4
					61.0 (m)		45.5
							48.6
poly-**3h**	CN	CH_3	H	3	56.3 (M)	4	37.4
					57.4 (m)		42.2
					59.5 (m)		45.9
							48.6
poly-**3i**	CN	H	CH_3	1	56.1	2	46.1
							49.1
poly-**3j**	C≡C-2-Pyr	H	H	2	57.1 (M)	5	39.2
					60.9 (m)		40.0
							42.2
							47.3
							49.8
poly-**3k**	$COOC_2H_5$	H	H	1	57.8	NO[e]	48.4 (M)
							50.8 (m)
poly-**3l** (poly-**BF1**)	$COOC_2H_5$	CH_3	H	1	57.5	NO[e]	47.9 (M)
							50.8 (m)
poly-**3ma**	COOH	CH_3	H	1	57.3	NO[e]	48.2
poly-**BF2**				*f*	57.8		43.8
poly-**BF1**				*g*	54.2		45.6
poly-**BF1**				*h*	63.1		30.2

[a] Number of ^{13}C NMR signals attributable to aliphatic quaternary carbon in position 1 of the indene moiety. [b] The ppm value of the ^{13}C NMR signal(s) attributable to the aliphatic quaternary carbon. [c] Number of cross-peaks attributable to backbone methylene in the HSQC spectrum. [d] The ppm value of the signal(s) attributable the backbone methylene ^{13}C. [e] NO = not observed. [f] See ref 10. [g] Calculated for 1,2-polymerization (see ref 12). [h] Calculated for 1,4-polymerization (see ref 12).

When the bulky electron-withdrawing $COOC_2H_5$ of poly-**3k,l** was replaced by a small donor methyl group in poly-**3f**, the ^{13}C signals attributable to the carbon atom of the backbone methylene and to the aliphatic quaternary carbon in position 1 of indene moiety of poly-**3f** were clearly doubled. It is noteworthy that the chemical shift values of the couple of signals attributable to the aliphatic quaternary carbon of poly-**3f** (57.4 and 61.0 ppm) were very close to those calculated for poly-**BF1** in the two different enchainments (54.2 and 63.1 ppm). Thus, in some monomeric units of poly-**3f** the indene double bond could be retained in the original position, while in some others it could be shifted as a consequence of a diene (1,4) polymerization.

On the other hand, several minor species are present in the ^{13}C NMR spectra of poly-**3g,h** (showing a nitrile group) and poly-**3c**−**e** showing a halogen atom. The number of the peaks attributable to aliphatic quaternary carbon and their chemical shift suggest the presence in these polymers of enchainment,

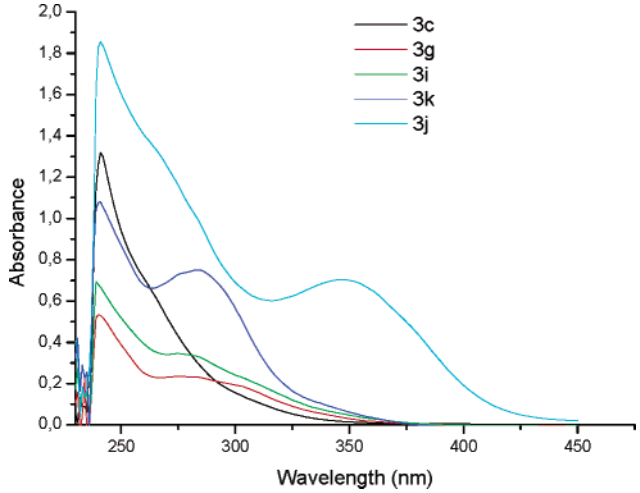

Figure 2. Comparison of the absorption spectra of poly-**3c,g,i**−**k**. The spectra were recorded at room temperature with polymer solutions showing the same concentrations (1.0×10^{-5} mol/L in chloroform) in monomer base unit.

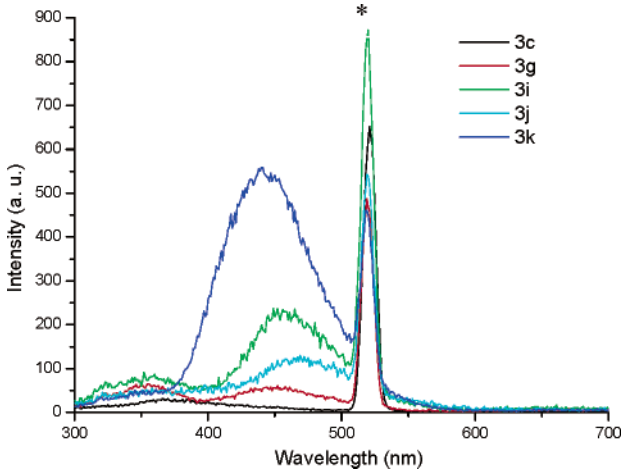

Figure 3. Comparison of the emission spectra of poly-**3c,g,i**−**k**. The spectra were performed in chloroform at room temperature with an excitation wavelength of 260 nm. The asterisk indicates the secondary scattering of the excitation beam.

configurational, and/or conformational isomers. The maximum of the complexity is reached in poly-**3a** (R_1 = H), which displays two broad peaks attributable to aliphatic quaternary carbon, while the signals attributable to backbone methylene are dispersed in a wide range of chemical shifts.

Poly-**3i** (R_1 = CN) represents a special case because, in spite of the presence in its monomeric unit of a small electron-withdrawing group in position 2 of the indene nucleus, it shows an evident analogy with the polymers bearing a bulkier electron-withdrawing ester group (poly-**3k,l**). This apparent discrepancy can be explained by the presence of a methyl group in the proximity of the reactive exocyclic methylene group in the monomer that seems to be capable of inhibiting diene (1,4) polymerization.

Finally, these results suggest that the steric hindrance in the proximity of the reactive exocyclic methylene group of the monomer affects the macromolecular structure of these polymers.

2.4.2. Absorption and Emission Spectroscopy. A comparative study of the absorption and emission spectra of the whole polymer set was performed in order to obtain information on the poly-**3** structure.

The comparison of the UV−vis absorption spectra (Figure 2) showed the existence of a common absorption component centered around 240−242 nm attributable to the 3-phenylindene moiety and a second component of variable intensity centered at about 270−284 nm. The second component was particularly evident in the polymers bearing an ester group in position 2 of the indene moiety (e.g. poly-**3k,l**), whereas it was less manifest in the polymer bearing a fluorine atom (poly-**3c**) and can be related to the presence of a more extended length of π-conjugation. (Indeed, an ethyl cinnamate moiety can be recognized in the monomeric unit of poly-**3k,l**.) Finally, poly-**3j** showed a third component centered at about 346 nm that could be explained with its even more extended conjugation.

It is generally assumed that the fluorescence in solution of a polymer with aromatic side groups is composed of monomer and excimer emissions. The emission spectrum of poly-**3a** (R_1 = H) showed two broad peaks, the first at about 370 nm and the second at about 460 nm. In the structurally related poly-**BF2**, Londergan and co-workers attributed the predominant emission at 448 nm to the formation of an excimer resulting from chromophore stacking, and the secondary peak at 347 nm to the monomer emission on the basis of the observation that 3-phenylindene (the model of the monomeric unit) showed an emission peak at 345 nm.[10] Poly-**BF1** (poly-**3l**) and closely related poly-**3k** showed a broad emission peak centered at 440 nm (Figure 3), while both models of poly-**BF1** monomeric units showed maximum emissions at about 380 nm.[12] These results allowed to attribute the emission of poly-**3** around 350−380 nm to nonstacked monomeric units and the peaks at 440−470 nm to the stacked ones with sufficient confidence.

On the basis of this assumption, the extent of the chromophore stacking in poly-**3** was highly variable. Thus, poly-**3a** (emitting at 370 and 460 nm) could be considered to be less stacked than both poly-**BF1** (emitting only at 440 nm) and poly-**BF2**, and poly-**3c**−**f** (emitting only at 360−380 nm) were even less stacked. Intermediate situations can be inferred from the spectra of poly-**3g**−**j**, which show variable proportions between the two emission components.

2.4.3. Mass Spectrometry. Matrix-assisted laser desorption ionization time-of-flight (MALDI-TOF) mass spectrometry of the poly-**3a,g**−**l** confirmed the structure of these polymeric materials. The MALDI spectra obtained with dithranol as a matrix showed the presence of a series of peaks differing by the molecular weight of the corresponding monomer up to a mass-to-charge ratio of about 4000−8000 depending on the structure of the polymer. Heavier polymeric species, having much lower ionization efficiency, were undetectable under these conditions (see for example Figure 4).

2.4.4. Differential Scanning Calorimetry. Samples of poly-**3** were characterized by differential scanning calorimetry (DSC) over a temperature range of 40−340 °C at a heating rate of 20 °C for the identification of potential solid state changes. The DSC analysis showed that the thermal behavior of these polymers is affected by the substituent present in position 2 of the indene moiety. In particular, poly-**3a** (R_1 = H) showed a flat DSC curve, while the halogen-containing polymers (e.g., poly-**3c**, R_1 = F; poly-**3d**, R_1 = Cl; poly-**3e**, R_1 = Br) showed broad endothermic peaks.

In the DSC curve of the polymer bearing a methyl group in position 2 of the indene nucleus (poly-**3f**), the endothermic peak becomes more evident, and in poly-**3k,l** (R = $COOC_2H_5$) the endothermic peak is very sharp (Figure 5).

However, the comparison of the DSC curve of poly-**3l** (poly-**BF1**) with the previously published DTGA (differential thermogravimetric analysis) curve (showing a peak at 240−250 °C)

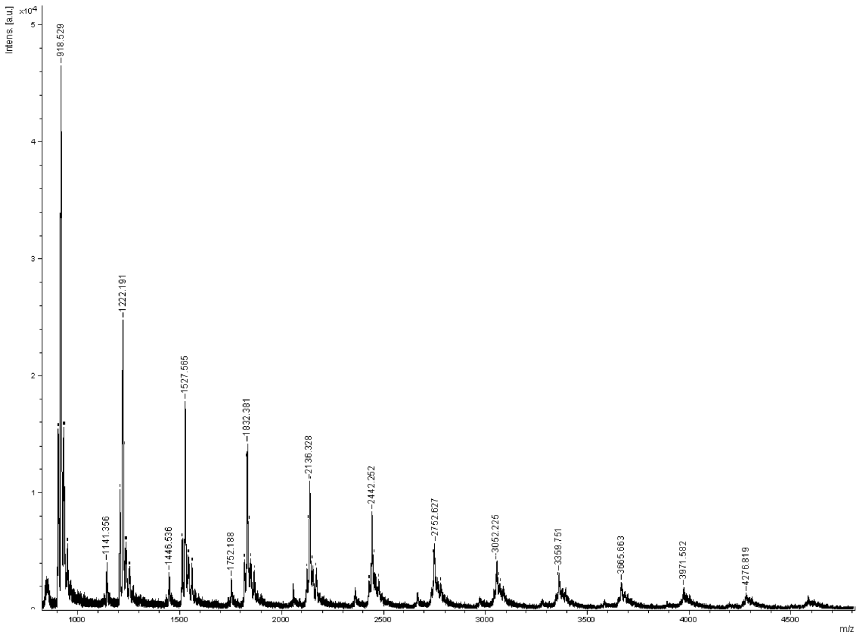

Figure 4. MALDI-TOF spectra of poly-**3j**.

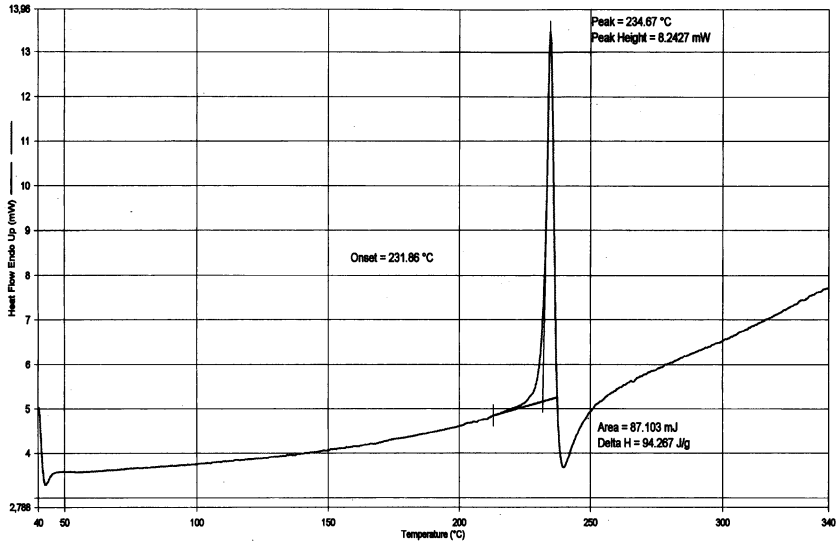

Figure 5. DSC curve of poly-**3l** (poly-**BF1**).

of the same polymer suggests that the endothermic peak at 235 °C could be related to the depolymerization process rather than to the polymer crystallinity.

The polymers bearing a cyano group (poly-**3g**−**i**) show more complex DSC curves, which are characterized by the presence of two endothermic peaks, whereas the poly-**3j** DSC is even more complex and difficult to explain.

On the basis of the above assumption, DSC analysis can be used to predict the depolymerization behavior (see below).

2.5. Thermoreversibility Analysis. The heating to reflux of the polymers solutions in solvents showing different boiling points led to both the depolymerization of poly-**3c**−**l,ma** and the regeneration of the corresponding benzofulvene monomers. On the basis on these findings, the depolymerization process was characterized by NMR spectroscopy at high temperature (experiments at different times in nitrobenzene-d_5 at 150 °C, see Table 4). By way of example, Figure 6 shows that the broad lines typical of poly-**3k** progressively disappear as a consequence of the exposure to high temperature to be replaced by the sharp signals of the benzofulvene monomer **3k**.

The results shown in Figure 6 suggest that the depolymerization of poly-**3k** can be considered nearly complete after 6 h heating at 150 °C. This result is in agreement with the previously described one obtained with closely related poly-**BF1** (poly-**3l**).[11]

On the contrary, the polymer bearing a hydrogen atom in position 2 of the indene moiety (poly-**3a**) fail to show any significant depolymerization after 24 h heating at the same temperature. Interestingly, the polymers bearing a cyano group in position 2 of the indene moiety (e.g., poly-**3g**−**i**) show a particular behavior because their depolymerization was detectable already at room temperature, rapid at 150 °C, but it was not completed after 24 h heating at the same temperature. For the polymers bearing an halogen atom (e.g., poly-**3c**−**e**) or a methyl group in position 2 of the indene moiety (poly-**3f**) the thermoinduced depolymerization appear to be slower, and equilibrium is reached in times variable from 3 to 24 h (Table 4).

In the latter polymers the equilibrium polymerization process is particularly evident, and more in general, the stereoelectronic

Table 4. Comparison of Some Significant DSC Features of the Synthesized Polymers with the Thermoinduced Depolymerization Followed by ^{1}H NMR Spectroscopy

polymer	R_1	R_2	R_3	peaks no. (appearance)	peaks temp (°C)	peaks ΔH (J/g)[a]	thermoinduced depolymerization at 150 °C by ^{1}H NMR[b]
poly-**3a**	H	H	H				no-depolymerization after 24 h
poly-**3c**	F	H	H	1 (broad)	202	24.4	equilibrium after 3 h
poly-**3d**	Cl	H	H	1 (broad)	276	51.5	equilibrium after 6−24 h
poly-**3e**	Br	H	H	1 (broad)	214	70.5	equilibrium after 3−6 h
poly-**3f**	CH_3	H	H	1 (broad)	242	88.5	equilibrium after 6−24 h
poly-**3g**	CN	H	H	2 (broad)	199	4.9	equilibrium after 0.25 h
					244	35.1	
poly-**3h**	CN	CH_3	H	2 (broad)	188	16.8	equilibrium after 0.25−1 h
					242	37.1	
poly-**3i**	CN	H	CH_3	3 (broad)	212	19.9	equilibrium after 0.25−1 h
					251	−7.5	
					327	16.3	
poly-**3j**	C≡C-2-Pyr	H	H				equilibrium after 1−3 h
poly-**3k**	$COOC_2H_5$	H	H	1 (sharp)	232	98.5	depolymerization almost complete after 3−6 h
poly-**3l** (poly-**BF1**)	$COOC_2H_5$	CH_3	H	1 (sharp)	235	94.3	depolymerization almost complete after 3−6 h

[a] The positive values refer to the endothermic peaks; the negative value is exothermic. [b] In the thermoreversibility experiments samples of the polymers (5 mg) were dissolved into nitrobenzene-d_5 (0.5 mL) and heated in an oil bath thermostated at 150 °C; the ^{1}H NMR experiments were performed at regular time intervals.

features of the substituents in position 2 of indene appear to play a key role in the process.

2.6. Aggregate Structure. The previously reported transmission electron microscopy (TEM) studies showed that freshly prepared poly-**BF1** formed several differently ordered nanostructured aggregates such as nanospheres (NS), small diameter knotted tubes (SDTK), large diameter knotted tubes (LDKT), small diameter three-dimensional nets (SDTN), and large-diameter three-dimensional nets (LDTN), whereas SDTN and LDTN were the main species detected in experiments performed with aged poly-**BF1**.[12]

On the basis of this intriguing result, the aggregate structure of the newly synthesized polymers (poly-**3**) was investigated by scanning electron microscopy (SEM) in order to assess the relationship between monomer and aggregate structures. The results of the initial study performed on poly-**BF1** showed a good agreement with the previously published ones obtained by TEM (Figure 7). More in general, benzofulvene polymers poly-**3** are liable to give differently ordered aggregates (Figure 8 shows some selected examples), but no clear relationship was found to exist between monomer and aggregate structures.

The most interesting observation was that polymers showing low molecular weight, like poly-**3a,** are particularly liable to give nanospheres characterized by favorable dimensions and morphology (Figure 9), whereas for polymers formed by a high number of monomeric units (e.g., poly-**3f,i**), larger fractal-like structures showing limited self-similarity are the main aggregate species detected (Figure 8).

3. Conclusion

A viable general method for the synthesis of new benzofulvene derivatives **3** was developed in order to prepare a series of differently substituted **3** in gram-scale amounts. Monomers **3** were characterized with respect to their capability of polymerizing spontaneously to give polymers based on functionalized indene monomeric units, and the results of this study suggest that the steric hindrance at position 2 of the indene moiety plays an important role in inhibiting spontaneous polymerization. Moreover, the steric hindrance in the close proximity of position 2 seems to be capable of affecting the molecular weight of the polymer molecules.

NMR spectroscopic studies show that the macromolecular structure of some newly synthesized polymers is rather complex with the possible presence of enchainment, configurational, and/or conformational isomers. Again, steric hindrance in the proximity of the reactive vinylene group of monomers **3** appears to play a major role in determining the macromolecular structure of these polymers. It is noteworthy that the simplest ^{13}C NMR spectra are shown by poly-**3k,l**, in which R_1 is a bulky electron-withdrawing $COOC_2H_5$ moiety, or by poly-**3i**, in which the small electron-withdrawing group R_1 (CN) is coupled to the presence of a methyl group in the proximity of the reactive exocyclic methylene. The stereoelectronic characteristics of the R_1 substituent affect also the photophysical features of poly-**3** and, in a special way, the fluorescence spectra, which show a variable proportion between two different emission components attributable to either nonstacked or stacked monomeric units. All the newly synthesized poly-**3** show a thermoreversible polymerization/depolymerization with the exception of the unsubstituted poly-**3a**. Preliminary ^{1}H NMR studies suggest that the polymerization/depolymerization equilibrium is affected by the stereoelectronic features of R_1 substituent, but further studies are required to define with precision the physicochemical constants of this equilibrium polymerization phenomenon. Finally, scanning electron microscopy (SEM) shows that low-molecular-weight polymer poly-**3a** is liable to give nanospheres, whereas polymers formed by a high number of monomeric units (e.g., poly-**3f,i**) demonstrate the tendency to aggregate in larger fractal-like structures showing limited self-similarity. In conclusion, these results suggest that the size of substituent R_1 appears to affect the supramolecular structure by affecting the molecular weight of the polymer.

4. Experimental Section

Synthesis. Melting points were determined in open capillaries in a Gallenkamp apparatus and are uncorrected. UV/vis spectra were recorded with a Shimadzu 260 spectrophotometer, and the emission spectra were performed by means of a Shimadzu RF-5001PC instrument. Merck silica gel 60 (230−400 mesh) was used for column chromatography. Merck TLC plates, silica gel 60 F254, were used for TLC. ^{1}H NMR spectra were recorded at 200 MHz (Bruker AC200 spectrometer), at 400 MHz (Bruker DRX-400 AVANCE spectrometer), or at 600 MHz (Bruker DRX-600 AVANCE spectrometer) in the indicated solvents (TMS as internal standard): the values of the chemical shifts are expressed in ppm and the coupling constants (J) in Hz.

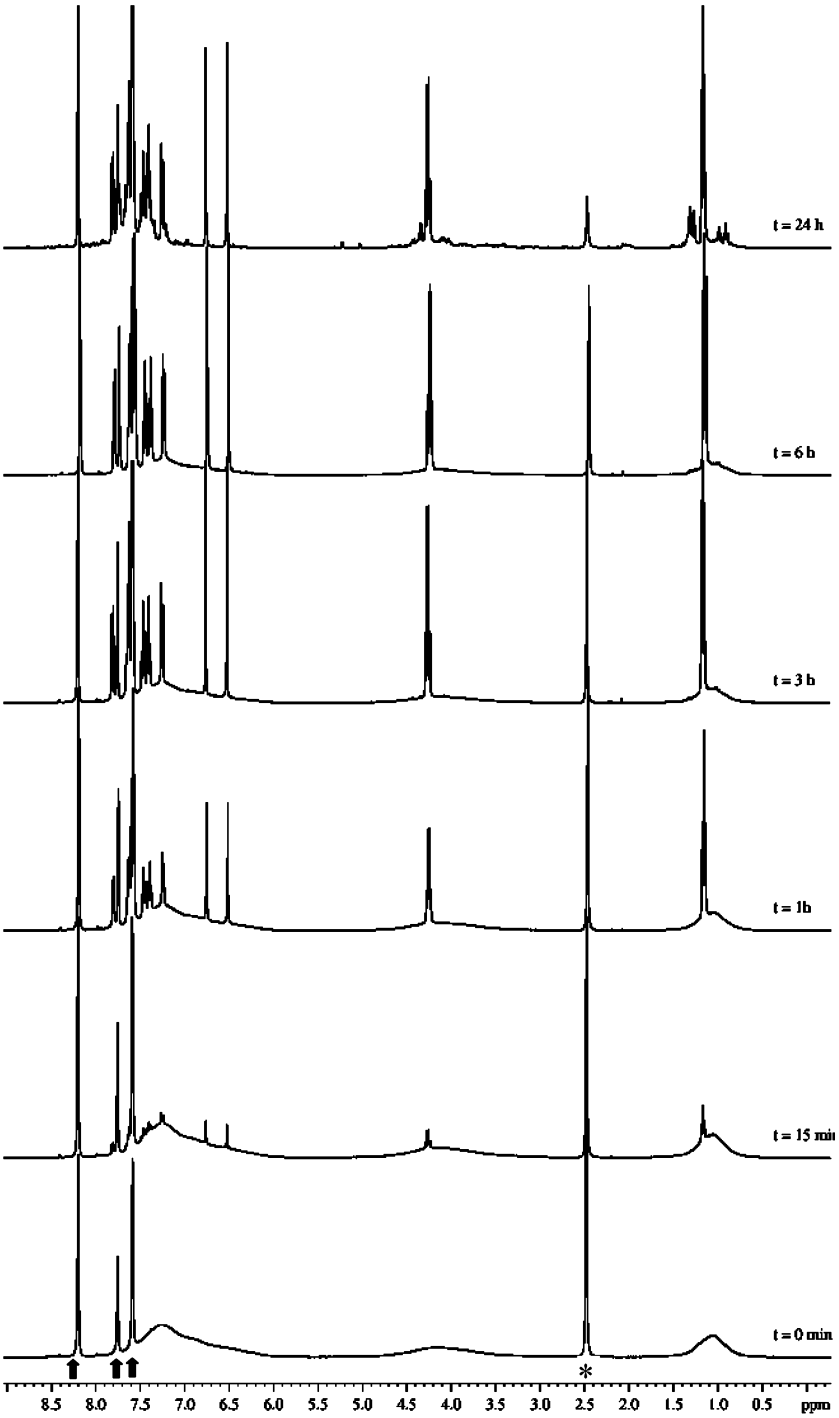

Figure 6. Thermoinduced depolymerization of poly-**3k**, followed by ^{1}H NMR (400 MHz). The arrows indicate the solvent (nitrobenzene) peaks. The asterisk indicates the water peak.

Size Exclusion Chromatography (SEC). The molecular characterization of polybenzofulvene derivatives was performed by a multiangle light scattering (MALS) photometer on-line to a SEC chromatographic system. The SEC-MALS system consisted of an Alliance chromatographic system from Waters (Milford, MA), a MALS Dawn DSP-F photometer from Wyatt (Santa Barbara, CA), and a differential refractometer (Waters model 410) used as concentration detector. The multidetector SEC-MALS system has been described in detail elsewhere.[17,18] The column set was composed of two mixed Styragel SEC columns (HR5E and HR4E) from Waters. The experimental conditions consisted of tetrahydrofuran (THF) as mobile phase, a temperature of 35 °C, and 0.8 mL/min flow rate. The calibration constant of the MALS photometer was calculated using toluene as standard assuming a Rayleigh Factor of 1.406×10^{-5} cm^{-1}. The MALS angular normalization was performed by measuring the scattering intensity of a very narrow low-molar-mass polystyrene standard ($M = 10.9$ kg/mol, $D \leq 1.03$) in the mobile phase which was assumed to act as an isotropic scatterer. The refractive index increment, d*n*/d*c*, of the polymer with respect to the mobile phase at 25 °C was measured by a KMX-16 differential refractometer from LDC Milton Roy (Rochester, NY).

NMR Spectroscopy. NMR experiments were performed with a Bruker DRX-600 AVANCE spectrometer, equipped with an *xyz* gradient unit, operating at 600.13 and 150.89 MHz for ^{1}H and ^{13}C, respectively. NMR data were processed by using the NMRpipe[19] software (version 3.3), and 2D spectra were analyzed with the SPARKY[20] software. Gradient-selected ^{1}H−^{13}C HSQC[21] spectra were acquired with 2048 complex points for 256 experiments with 2 s recycle. $^1J_{CH}$ was fixed at 145 Hz.

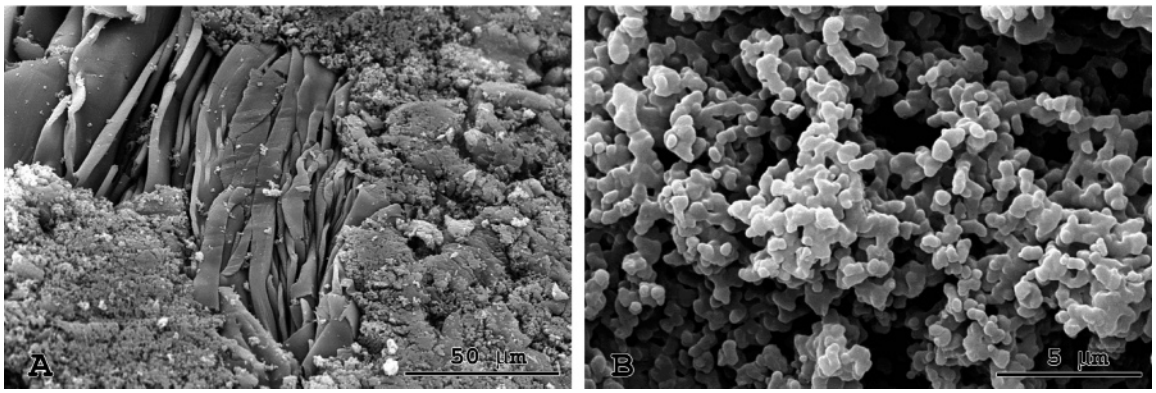

Figure 7. SEM micrograph of freshly prepared poly-**3l** (poly-**BF1**).

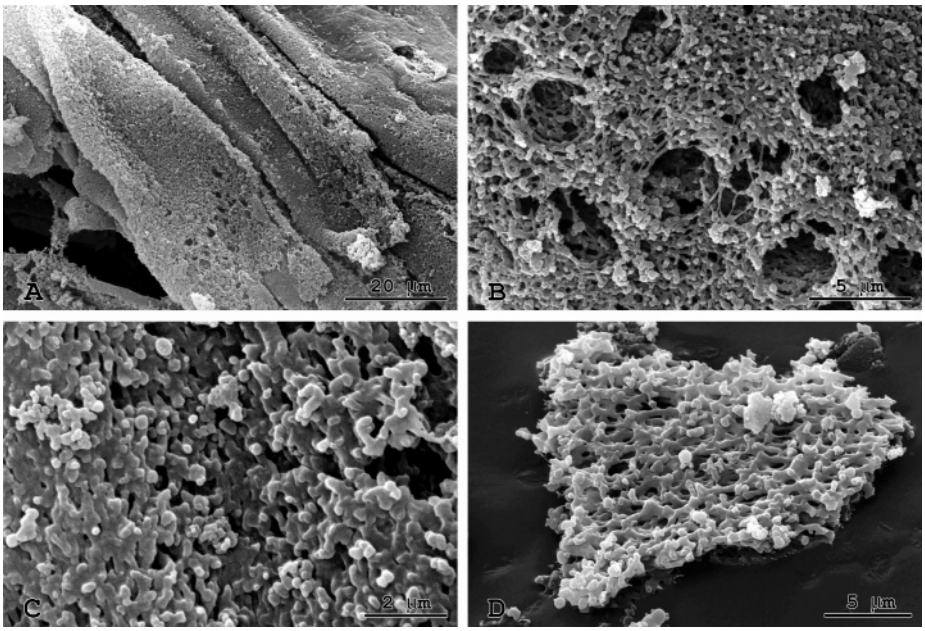

Figure 8. SEM micrograph of freshly prepared poly-**3f** (A-C) and poly-**3i** (D).

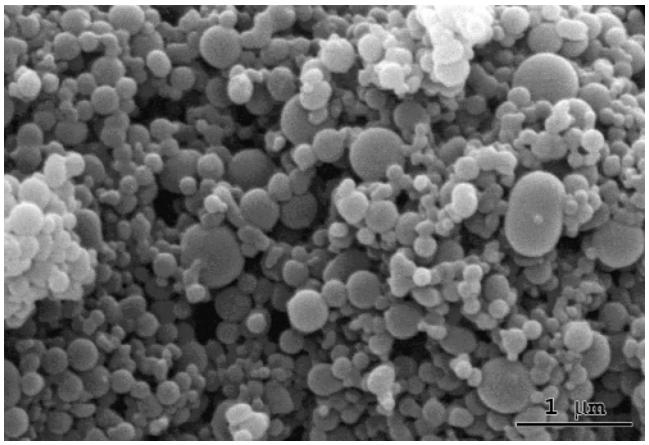

Figure 9. SEM micrograph of freshly prepared poly-**3a**.

Mass Spectrometry. Mass spectra of intermediate compounds and monomers were obtained by using GC-MS and electrospray ionization. In the former case, a Varian Saturn 2000 ion trap coupled with a Varian 3800 gas chromatograph (Varian, Walnut Creek, CA), equipped with a J&W DB5-MS column (30 m × 0.25 mm, film thickness 0.25 μm), was used. The instrument was operating in electron ionization mode at 70 eV with a source temperature of 150 °C. Electrospray ionization has been obtained by a LCQ DECA mass spectrometer (ThermoFinnigan, Waltham, MA) operating in positive mode with a capillary voltage of 4.6 kV.

The mass spectrometry characterization of polybenzofulvene derivatives has been carried out by a Ultraflex MALDI-TOF/TOF (Bruker Daltonics, Bremen, Germany) instrument. 10 mL of a $CHCl_3$ solution of the polymer (10 mg/mL) was mixed with 1,8,9-trihydroxyanthracene (Dithranol, Fluka) as a matrix and submitted to the N_2 (337 nm) laser desorption.

Differential Scanning Calorimetry. Differential scanning calorimetric (DSC) analysis was performed with a Perkin-Elmer DSC-7 instrument and PYRIS software (version-5). The temperature axis and the cell constant were calibrated with indium. Weighed samples of poly-**3** in pin-holed aluminum pans were heated at 20 °C/min over a temperature range of 40−340 °C under nitrogen purge (20 mL/min).

X-ray Crystallography. Single crystals of **1f**,**i**,**o**, **2f**,**j**,**m**,**p**, **3n**-PTSA, and **5h** were submitted to X-ray data collection on a Siemens P4 four-circle diffractometer with graphite monochromated Mo Kα radiation (λ = 0.710 69 Å). The $\omega/2\Theta$ scan technique was used. The structures were solved by direct methods, and the refinements were carried out by full-matrix anisotropic least-squares of F^2 against all reflections. The hydrogen atoms were located on Fourier difference maps or placed in calculated positions and included in the structure factor calculations with isotropic temperature factor. Atomic scattering factors including f' and f'' were taken from ref 22. Structure solution was carried out by SHELXS-97.[23] Structure refinement and molecular graphics were performed by SHELX-97[22] and the WinGX package,[24] respectively.

CCDC 628326 (**1f**), 628323 (**1i**), 628325 (**1o**), 628327 (**2f**), 628328 (**2j**), 628321 (**2m**), 612948 (**2p**), 628324 (**3n**-PTSA), and

628322 (**5h**) contain the supplementary crystallographic data for this paper. These data can be obtained free of charge via www.ccdc.cam.ac.uk/conts/retrieving.html (or from the Cambridge Crystallographic Data Centre, 12 Union Road, Cambridge CB2 1EZ, UK; fax: (+44) 1223-336-033; or e-mail: deposit@ccdc.cam.ac.uk).

Scanning Electron Microscopy (SEM). The material was mounted on aluminum holders by carbon-conductive glue and coated with 20 nm gold in a Balzer's MED 010 sputtering device. The samples were then observed with a Philips XL20 scanning electron microscope operating at an accelerating voltage of 20 kV.

Acknowledgment. Thanks are due to Italian MUR (Ministero dell'Università e della Ricerca) for financial support. Prof. Stefania D'Agata D'Ottavi's careful reading of the manuscript and Dr. Roberto Beretta's and Mr. Giulio Zannoni's technical assistance are also acknowledged. Gianluca Giorgi thanks Dr. Guido Mastrobuoni and Prof. Gloriano Moneti (C. I. S. M., Università di Firenze) for MALDI-TOF spectra.

Supporting Information Available: Full experimental details for the synthesis and the characterization of the new benzofulvene monomers, polymers, as well as their intermediates (chemistry, NMR, MS, X-ray structure). This material is available free of charge via the Internet at http://pubs.acs.org.

References and Notes

(1) Nakano, T.; Takewaki, K.; Yade, T.; Okamoto, Y. *J. Am. Chem. Soc.* **2001**, *123*, 9182−9183.
(2) Nakano, T.; Yade, T. *J. Am. Chem. Soc.* **2003**, *125*, 15474−15484.
(3) Nakano, T.; Yade, T.; Fukuda, Y.; Yamaguchi, T.; Okumura, S. *Macromolecules* **2005**, *38*, 8140−8148.
(4) Nakano, T.; Nakagawa, O.; Tsuji, M.; Tanikawa, M.; Yade, T.; Okamoto, Y. *Chem. Commun.* **2004**, 144−145.
(5) Nakano, T. Heat-Decomposable Polymer, WO03095523.
(6) Nakano, T. Polymer Having Unique Optical Property and Polymerizable Monomer thereof, US2004132963.
(7) Nakano, T. Optically Active High-Molecular Compounds, US200523-4267.
(8) Nakano, T.; Yade, T.; Yokoyama, M.; Nagayama, N. *Chem. Lett.* **2004**, 296−297.
(9) Ilhan, F.; Rotello, V. M. *J. Org. Chem.* **1999**, *64*, 1455−1458.
(10) Londergan, T. M.; Teng, C. J.; Weber, W. P. *Macromolecules* **1999**, *32*, 1111−1114.
(11) Cappelli, A.; Pericot Mohr, G.; Anzini, M.; Vomero, S.; Donati, A.; Casolaro, M.; Mendichi, R.; Giorgi, G.; Makovec, F. *J. Org. Chem.* **2003**, *68*, 9473−9476.
(12) Cappelli, A.; Anzini, M.; Vomero, S.; Donati, A.; Zetta, L.; Mendichi, R.; Casolaro, M.; Lupetti, P.; Salvatici, P. Giorgi, G. *J. Polym. Sci., Part A* **2005**, *43*, 3289−3304.
(13) Cappelli, A.; Pericot Mohr, G.; Giuliani, G.; Galeazzi, S.; Anzini, M.; Mennuni, L.; Ferrari, F.; Makovec, F.; Kleinrath, E. M.; Langer, T.; Valoti, M.; Giorgi, G.; Vomero, S. *J. Med. Chem.* **2006**, *49*, 6451−6464.
(14) Larock, R. C.; Doty, M. J. *J. Org. Chem.* **1993**, *58*, 4579−4583.
(15) Marsili, A. *Ann. Chim.* **1961**, *51*, 237−251.
(16) Koelsch, C. F. *J. Org. Chem.* **1960**, *25*, 2088−2091.
(17) Mendichi, R.; Giacometti Schieroni, A. In *Current Trends in Polymer Science*; Pandalai, S. G., Ed.; Trans-World Research Network: Trivandrum, India, 2001, Vol. 6, pp 17−32.
(18) Wyatt, P. J. *Anal. Chim. Acta* **1993**, *272*, 1−40.
(19) Delaglio, F.; Grzesiek, S.; Vuister, G.; Zhu, G.; Pfeifer, J.; Bax, A. *J. Biomol. NMR* **1995**, *6*, 277−293.
(20) Goddard, T. D.; Kneller, D. G. SPARKY 3 package, University of California, San Francisco.
(21) Bax, A.; Subramanian, S. *J. Magn. Reson.* **1988**, *67*, 565−569.
(22) Sheldrick, G. SHELXL-97, A Program for Crystal Structure Refinement, University of Gottingen, Gottingen (Germany), Release 97-2, 1997.
(23) Sheldrick, G. SHELXS-97, A Program for Automatic Solution of Crystal Structures, University of Gottingen, Gottingen (Germany), Release 97-2, 1997.
(24) Farrugia, L. J. *J. Appl. Crystallogr.* **1999**, *32*, 837.

MA0629236